THE JOURNAL OF BIOLOGICAL CHEMISTRY VOL. 283, NO. 20, pp. 14041–14052, May 16, 2008

A Novel GDP-dependent Pyruvate Kinase Isozyme from *Toxoplasma gondii* Localizes to Both the Apicoplast and the Mitochondrion*

Received for publication, November 2, 2007, and in revised form, March 3, 2008 Published, JBC Papers in Press, March 6, 2008, DOI 10.1074/jbc.M709015200

Tomoya Saito[‡1], Manami Nishi[§1], Muoy I. Lim[§], Bo Wu[§], Takuya Maeda[‡], Hisayuki Hashimoto[‡], Tsutomu Takeuchi[‡], David S. Roos[§2], and Takashi Asai[‡3]

From the [‡]Department of Tropical Medicine and Parasitology, Keio University School of Medicine, 35 Shinanomachi, Shinjuku-ku, Tokyo 160-8582, Japan and the [§]Department of Biology, University of Pennsylvania, Philadelphia, Pennsylvania 19104

We previously reported a cytosolic pyruvate kinase (EC 2.7.1.40) from *Toxoplasma gondii* (*Tg*PyKI) that differs from most eukaryotic pyruvate kinases in being regulated by glucose 6-phosphate rather than fructose 1,6-diphosphate. Another putative pyruvate kinase (*Tg*PyKII) was identified from parasite genome, which exhibits 32% amino acid sequence identity to *Tg*PyKI and retains pyruvate kinase signature motifs and amino acids essential for substrate binding and catalysis. Whereas *Tg*PyKI is most closely related to plant/algal enzymes, phylogenetic analysis suggests a proteobacterial origin for *Tg*PyKII. Enzymatic characterization of recombinant *Tg*PyKII shows a high pH optimum at 8.5, and a preference for GDP as a phosphate recipient. Catalytic activity is independent of K^+, and no allosteric or regulatory effects were observed in the presence of fructose 1,6-diphosphate, fructose 2,6-diphosphate, glucose 6-phosphate, ribose 5-phosphate, AMP, or ATP. Unlike *Tg*PyKI, native *Tg*PyKII activity was exclusively associated with the membranous fraction of a *T. gondii* tachyzoite lysate. *Tg*PyKII possesses a long N-terminal extension containing five putative start codons before the conserved region and localizes to both apicoplast and mitochondrion by immunofluorescence assay using native antibody and fluorescent protein fusion to the N-terminal extension. Further deletional and site-directed mutagenesis suggests that a translation product from 1st Met is responsible for the localization to the apicoplast, whereas one from 3rd Met is for the mitochondrion. This is the first study of a potential mitochondrial pyruvate kinase in any system.

Toxoplasma gondii is an obligate intracellular protozoan parasite of warm-blooded animals, including humans (1). Although normally asymptomatic, toxoplasmosis is a significant problem in pregnant women infected early during gestation, immunocompromised individuals, and livestock. This parasite is a member of the phylum Apicomplexa, which includes many other parasites such as *Plasmodium* species responsible for malaria. Glucose is thought to be the main source of energy for the rapidly multiplying forms of both *Toxoplasma* and *Plasmodium*, which use the Embden-Meyerhof pathway for glycolytic phosphorylation (2).

Pyruvate kinase catalyzes the essentially irreversible transphosphorylation from phosphoenolpyruvate (PEP)[4] to ADP-producing pyruvate (3). In most mammals and bacteria, pyruvate kinase is allosterically regulated by fructose 1,6-diphosphate (4) and thus plays a regulatory role in glycolysis. The product pyruvate feeds into many metabolic pathways, placing pyruvate kinase at a crucial metabolic intersection. Many organisms express multiple pyruvate kinase isozymes with different kinetic properties. For example, *Escherichia coli* bears two isozymes, type I and II, both of which are homotropically activated by the substrate PEP. The type I isozyme is also activated heterotropically by fructose 1,6-diphosphate and is inhibited by ATP (5), whereas the type II isozyme is activated by AMP and monophosphorylated sugars (6). Pyruvate kinases are expressed in the cytosol in most organisms. Plants and algae have additional isozymes in chloroplasts with markedly different physical and kinetic/regulatory characteristics (7).

We have previously described the kinetic and regulatory properties of the cytosolic *T. gondii* pyruvate kinase (*Tg*PyKI). Unlike *T. gondii* hexokinase (8) and phosphofructokinase (9) that lack allosteric regulation, *Tg*PyKI is allosterically regulated by glucose 6-phosphate (10, 11), suggesting an important role in the control of glycolysis. We recently identified a second,

* This work was supported, in whole or in part, by National Institutes of Health grants. This work was also supported by Grant-in-aid for Scientific Research (KAKENHI) for Young Scientists (B) from the Ministry of Education, Culture, Sports, Science, and Technology 15790217, a Keio University grant-in-aid for encouragement of young medical scientists, and a Keio University special grant-in-aid for innovative collaborative research projects. The costs of publication of this article were defrayed in part by the payment of page charges. This article must therefore be hereby marked "*advertisement*" in accordance with 18 U.S.C. Section 1734 solely to indicate this fact.

The nucleotide sequence(s) reported in this paper has been submitted to the GenBank™/EBI Data Bank with accession number(s) AB118155.

[1] Both authors contributed equally to this work.

[2] Senior Scholar in Global Infectious Diseases of the Ellison Medical Foundation.

[3] To whom correspondence should be addressed: Dept. of Tropical Medicine and Parasitology, Keio University School of Medicine, 35 Shinanomachi, Shinjuku-ku, Tokyo 160-8582, Japan. Tel.: 81-3-3353-1211 (Ext. 62747); Fax: 81-3-3353-5958; E-mail: asait@sc.itc.keio.ac.jp.

[4] The abbreviations used are: PEP, phosphoenolpyruvate; ACP, acyl carrier protein; *Tg*PyK, *T. gondii* pyruvate kinase; YFP, yellow fluorescent protein; SA, predicted signal anchor; SP signal peptide; pTP, predicted plastid transit peptide; mTP, predicted mitochondrion targeting peptide; aa, amino acid; CHES, 2-(cyclohexylamino)ethanesulfonic acid; bis-Tris, 2-[bis(2-hydroxyethyl)amino]-2-(hydroxymethyl)propane-1,3-diol; MOPS, 4-morpholinepropanesulfonic acid; PBS, phosphate-buffered saline; Ab, antibody; HA, hemagglutinin; MES, 2-(*N*-morpholino)ethanesulfonic acid; HFF, human foreskin fibroblast; IFA, immunofluorescence assay; ER, endoplasmic reticulum; TES, 2-{[2-hydroxy-1,1-bis(hydroxymethyl)ethyl]amino}ethanesulfonic acid; NDP, nucleoside diphosphate; RFP, red fluorescent protein.

highly diverged isozyme in *T. gondii* EST and genome data bases (12, 13). This study describes the molecular genetic characterization, phylogeny, recombinant expression/purification, kinetic characterization, and subcellular localization of this *T. gondii* pyruvate kinase isozyme (*Tg*PyKII).

EXPERIMENTAL PROCEDURES

Parasites, Host Cells, Chemicals, and Reagents—RH strain *T. gondii* tachyzoites were maintained by serial passage in primary human foreskin fibroblasts (HFF) in Eagle's minimum essential media (Invitrogen) containing 1% heat-inactivated fetal bovine serum (Ed1 media) (14) or in mouse peritoneal fluid (15). Construction of parasites stably expressing p*tub*FNR_L-yellow fluorescent protein (YFP)-HA (labeling the apicoplast) and p*tub*$HSP60_L$-RFP (labeling the mitochondrion) is described elsewhere (16). PEP, phosphorylated sugars, nucleotides, potassium ferricyanide, and amino acids were obtained from Sigma. Rabbit polyclonal anti-acyl carrier protein (ACP) antibody was kindly provided by Drs. G. I. McFadden and R. F. Waller (17). MitoTrackerRed CMXRos (8-(4′-chloromethyl) phenyl-2,3,5,6,11,12,14,15-octahydro-1*H*,4*H*,10*H*,13*H*-diquinolizino-8*H*-xanthylium chloride), and Alexa Fluor Marina Blue/361 and 594-conjugated goat anti-rabbit antibodies were obtained from Invitrogen.

Cloning and Sequencing of TgPyKII cDNA—The following PCR primers were designed based on *T. gondii* ESTs CB030989, CB030879, and BI921053 (8): 5′-TGCAGAAATCGTCGCGCCGCAGCG-3′ (sense) and 5′-GCCGTGCTTGCCTTCTTTGG-3′ (antisense). PCR amplification of a *T. gondii* RH tachyzoite λZAP-II cDNA library (kindly provided by Dr. J. Ajioka, Cambridge University, UK) yielded a product with the expected size of 371 bp, which was used as a probe for cDNA library screening (8). Positive clones were sequenced on both strands using a Genetic Analyzer model 310 and 3700 (Applied Biosystems, Tokyo, Japan). The composite cDNA sequence was used for BLAST query against ToxoDB (18) to identify gene model TgTigrScan_6611. To confirm the 5′ end of the *Tg*PyKII cDNA, total RNA was extracted from RH strain of *T. gondii* tachyzoites (RNAqueous, Ambion, TX), and cDNA was amplified using GeneRacer kit (Invitrogen). 5′-rapid amplification of cDNA ends was performed using a gene-specific primer 5′-CACGTAGACAGAGGTGACGCTTCGGGG-3′. The complete cDNA sequence was analyzed by VectorNTI software (InforMax, Bethesda). The protein domains, families, and functional sites were analyzed using PROSITE (19). Signal properties were analyzed using TargetP (20, 21), SignalP (21, 22), and ChloroP (23) softwares. Hydrophobicity was examined using the Kyte and Doolittle procedure (24).

Phylogenetic Analysis—Twenty nine pyruvate kinase sequences from 20 taxa were extracted from GenBank™ and the OrthoMCL data base (25, 26) (see Fig. 2 legend for GenBank™ accession number), and aligned using ClustalX 1.83 (27), with manual curation. Regions of uncertain alignment were omitted, leaving 333 amino acid positions for analysis. Maximum likelihood trees were constructed using PROML from the PHYLIP 3.6a3 package (28), with 100 replicates, global rearrangement, and randomized input order options in conjunction with estimated parameter γ and the proportion of invariable sites obtained from TREE-PUZZLE5.1 (29). Bayesian analysis (30, 31) was carried out using MrBayes 3.0 with the JTT amino acid substitution model and 200,000 search generations.

Expression and Purification of Recombinant TgPyKII—An open reading frame predicted to encode the conserved region (from amino acid 293 to 988) of *Tg*PyKII was amplified using primers 5′-TAC<u>GGATCC</u>CTCTCTGCTGCGTCGCCC-3′ (sense) and 5′-TCG<u>GGATCC</u>**CTA**TCGCCCTGACTCGAGAGT-3′ (antisense), and cloned into the BamHI site of vector pGEX-6p-1 (Amersham Biosciences). Expression of the glutathione *S*-transferase-*Tg*PyKII-(293–988) fusion protein in *E. coli* BL21 was induced with 0.5 mM isopropyl β-thiogalactoside for 2.5 h, and purification of recombinant *Tg*PyKII was carried out by affinity chromatography on glutathione-Sepharose 4B (Amersham Biosciences), followed by treatment with PreScission Protease (Amersham Biosciences). The protein was applied to a DEAE-Toyo Pearl 650s column (TOSOH, Tokyo, Japan) equilibrated with 10 mM Tris-Cl, pH 8.0, containing 1 mM EDTA. Peak fractions eluted with a linear 0–500 mM gradient of KCl were pooled, concentrated, assayed for purity and concentration, and stored in 30% glycerol (w/v) at −80 °C. The protein concentration was determined by the dye-binding procedure described by Bradford (32) using bovine serum albumin as a standard. The purity of recombinant pyruvate kinase was analyzed by electrophoresis on 5–10% acrylamide gel. The protein was detected by Coomassie Brilliant Blue R-250 staining.

Enzyme Assays—Pyruvate kinase activity was determined by lactate dehydrogenase-coupled spectrophotometric assay (32), whereas monitoring oxidation of NADH due to pyruvate reduction at 340 nm was by using a UV-1600 spectrophotometer equipped with a TCC-240A temperature-controlled cell (Shimazu Co, Kyoto, Japan). 1-ml standard reaction mixture for assaying *Tg*PyKII activity contained 1 mM PEP, 0.5 mM GDP, 25.5 mM $MgCl_2$, 0.2 mM NADH, 20 units of rabbit muscle lactate dehydrogenase type II (Sigma), 100 mM Tris-Cl, pH 8.5, and 10–20 ng of the test enzyme. For substrate specificity studies, $MgCl_2$ was added in 25 mM excess of NDP to ensure formation of the $MgNDP^{2-}$ complex. All reactions were initiated by the addition of the substrate NDP. For determining optimal pH of recombinant *Tg*PyKII, MES, Tris-Cl, or CHES/NaOH buffers were used to generate a pH range from 6.0 to 10.0. Activities of *Tg*PyKI and succinate dehydrogenase were assayed as described previously (10, 11). All assays were carried out in triplicate at 37 °C. Reactions were monitored for 5 min, and the initial velocity was calculated from a tangent fitted to the reaction curve. Kinetic data were calculated using a nonlinear curve fitting algorithm (SigmaPlot 2000 software; SPSS Inc., Chicago).

Subcellular Fractionation of T. gondii Tachyzoites—10^{10} tachyzoites were washed twice and resuspended in TES homogenization buffer (250 mM sucrose, 1 mM EDTA, 5 mM triethanolamine-HCl, pH 7.5) and disrupted by French press at 35 kg/cm^2. After sedimentation of unbroken cells (~10%) at 2250 × *g* for 10 min, the supernatant was centrifuged for 20 min at 20,000 × *g* to yield a cytosolic (supernatant) and membranous (pellet) fractions. The pellet was washed once, resuspended in 1% Triton X-100 in TES buffer, and mechanically homogenized using a polychlorotrifluoroethylene homogenizer.

Native Antibody Production and Immunoblotting—Recombinant *Tg*PyKII-(293–988) purified from *E. coli* was used to immunize New Zealand White rabbits. Following three 50-μg injections at 2-week intervals, whole IgG was isolated from serum, and anti-*Tg*PyKII IgG was affinity-purified using CNBr-activated Sepharose 4B (Amersham Biosciences), which couples recombinant *Tg*PyKII-(293–988) as described previously (33). To check the cross-reactivity of anti-*Tg*PyKII to *Tg*PyKI, 3 ng of recombinant *Tg*PyKI (11) and recombinant *Tg*PyKII were loaded on 8% gradient polyacrylamide gel, which was then transferred to a Nitrocellulose Hybond-C extra membrane (Amersham Biosciences) using a semidry blotting apparatus. The membrane was blocked for 20 min with 2% skimmed milk in phosphate-buffered saline (PBS) containing 0.2% Tween 20 and incubated for 1 h with anti-*Tg*PyKII antibody (1:25 in blocking solution). Following washes in PBS with 0.2% Tween 20, the membrane was incubated with alkaline phosphatase goat anti-rabbit IgG (1:3000) (Vector Laboratories) for 1 h, following detection with a 5-bromo-4-chloro-3-indolyl phosphate-nitro blue tetrazolium system (Roche Applied Science). The molecular sizes of protein bands were determined with reference to pre-stained SDS-gel electrophoresis standards (Bio-Rad). To detect endogenous *Tg*PyKII expressed in *T. gondii*, 10^8 RH tachyzoites released from HFF monolayer were filtered through 3-μm pore-size Nuclepore polycarbonate filters (Whatman) and pelleted by centrifugation at 900 $\times$ *g* for 12 min. Parasites were lysed in PBS, containing NuPAGE LDS sample buffer (Invitrogen) and 0.5 M dithiothreitol. After denaturation at 70 °C for 10 min, parasite lysates were loaded on bis-Tris, 4–12% polyacrylamide gels (Invitrogen), and protein gel electrophoresis was performed using NuPAGE system with MOPS/SDS running buffer (Invitrogen). Proteins were transferred to nitrocellulose membrane using a Trans-Blot SemiDry apparatus (Bio-Rad), which was then blocked with 5% nonfat dry milk and 3% fetal bovine serum in PBS. The membrane was incubated for 1 h with a rabbit anti-*Tg*PyKII Ab (1:25 dilution) in blocking solution containing 0.2% Tween 20 (Sigma). Following washes in PBS with 0.2% Tween 20, the membrane was incubated for 1 h with a horseradish peroxidase-conjugated goat anti-rabbit secondary antibody (Bio-Rad) (1:2500 dilution) in blocking solution containing 0.2% Tween 20. Chemiluminescence reaction was performed using ECL Western blotting detection reagents (Amersham Biosciences), and blots were exposed on Kodak BioMax film.

Plasmid Construction—N-terminal 357 amino acids of *Tg*PyKII (unconserved region containing five possible start codons) from 1st Met were amplified from a *T. gondii* RH cDNA using primers (note that restriction enzyme site is underlined and start codon is boldface) 5′-CATCGC<u>AGATCT</u>**ATG**GACGATGGTGGAGCAGAGT-3′ (sense) and 5′-CGTCAC<u>ACTAGT</u>CGGTCCGATGGTTGC-3′ (antisense) and subcloned into BglII/AvrII sites of the *T. gondii* expression vector p*tub* or p*min*PT_F-YFP-HA (16)[5] to produce p*tub*/p*minTg*PyKII1stM-(1–357)-YFP-HA. DNA fragments from each downstream four start codons were generated using p*tub*/p*minTg*PyKII1stM-(1–357)-YFP-HA as a template, the above antisense primer, and the following sense primers: 5′-CATCGC<u>AGATCT</u>**ATG**AACTTTCCAACTTGT-3′ (from 2nd Met); 5′-CATCGC<u>AGATCT</u>**ATG**GCGCCTCTCCGACCC-3′ (from 3rd Met); 5′-CATCGC<u>AGATCT</u>**ATG**GATTTTCCACGGGTG-3′ (from 4th Met); or 5′-CATCGC<u>AGATCT</u>**ATG**CTCTCTGCTGCGTCG-3′ (from 5th Met). Plasmids p*tub*/p*minTg*PyKII2ndM-(19–357)-YFP-HA, p*tub*/p*minTg*PyKII3rdM-(93–357)-YFP-HA, p*tub*/p*minTg*PyKII4thM-(122–357)-YFP-HA, and p*tub*/p*minTg*PyKII5thM-(293-357)-YFP-HA were constructed using above described subcloning method. To introduce a point mutation, methionine to alanine, at 2nd or 3rd Met, site-directed mutagenesis was performed using QuikChange site-directed mutagenesis kit (Stratagene, CA). The plasmid p*tub*/p*min*PyKII1stM-(1–357)-YFP-HA was used as a template in the PCR by utilizing the following sets of primers (mutated amino acids are lowercase): 5′-GCTAATGGTTTTGCCAGCgcGAACTTTCCAACTTGTGG-3′ and 5′-CCACAAGTTGGAAAGTTCgcGCTGGCAAAACCATTAGC-3′ to produce p*tub*/*min*PyKII[2ndM19A]-YFP-HA, and 5′-CTCCTTCTCTCCGCGgcGGCGCCTCTCCGACC-3′ and 5′-GGTCGGAGAGGCGCCgcCGCGGAGAGAAGGAG-3′ to produce p*tub*/*min*PyKII[3rdM93A]-YFP-HA.

Parasite Transfection, Immunofluorescence Assay, and Fluorescent Microscopy—Parasite transfection was performed by electroporation as described previously (14). Parasites were inoculated onto glass coverslips (22 mm in diameter) with a confluent monolayer of HFF cells and incubated in a humidified 37 °C incubator for 24 h. Following a wash with PBS, coverslips were fixed with 3.7% paraformaldehyde in PBS, pH 7.0, for 5 min, permeabilized with 0.25% Triton X-100 in PBS, pH 7.0, for 10 min, and blocked for 30 min in a blocking solution (3% bovine serum albumin (fraction V, Fisher) and 5% fetal bovine serum in PBS, pH 7.0). For MitoTracker labeling, coverslips were incubated with 150 nM MitoTrackerRed CMXRos (Invitrogen) for 30 min and washed twice with Ed1 media before fixation. For immunofluorescence assay (IFA), coverslips were incubated with primary antibodies (anti-*Tg*PyKII Ab at 1:25 dilution or anti-ACP Ab at a 1:2000 dilution in blocking solution) for 1 h. Coverslips were washed three times with 0.25% Triton X-100 in PBS, and primary antibodies were detected either with Alexa Fluor Marina Blue/361-conjugated (1:500 dilution) or 594-conjugated goat anti-rabbit antibodies (1:4000 dilution) (Invitrogen) in the blocking solution for 1 h. After two washes with 0.25% Triton X-100 in PBS and a wash with PBS, the coverslips were mounted on glass slides using Fluoromount-G (SouthernBiotech, AL). To find out the localization of endogenous *Tg*PyKII, parasites stably expressing FNR_L-YFP-HA were labeled with MitoTracker Red CMXRos and subjected to IFA using anti-*Tg*PyKII and Alexa Fluor Marina Blue/361-conjugated goat anti-rabbit antibodies (Invitrogen). For examination of deletional constructs, wild type RH parasites were transfected, labeled with MitoTracker Red CMXRos, and subjected to IFA with anti-ACP and Alexa Fluor Marina Blue/361-conjugated goat anti-rabbit antibodies. Point mutational constructs were transfected either to wild type RH parasites that are subsequently labeled with anti-ACP and Alexa Fluor 594-conjugated goat anti-rabbit antibodies (Invitrogen) or to parasites stably expressing p*tub*$HSP60_L$-RFP.

[5] M. Nishi, C. He, O. Harb, J. Murray, and D. Roos, manuscript in preparation.

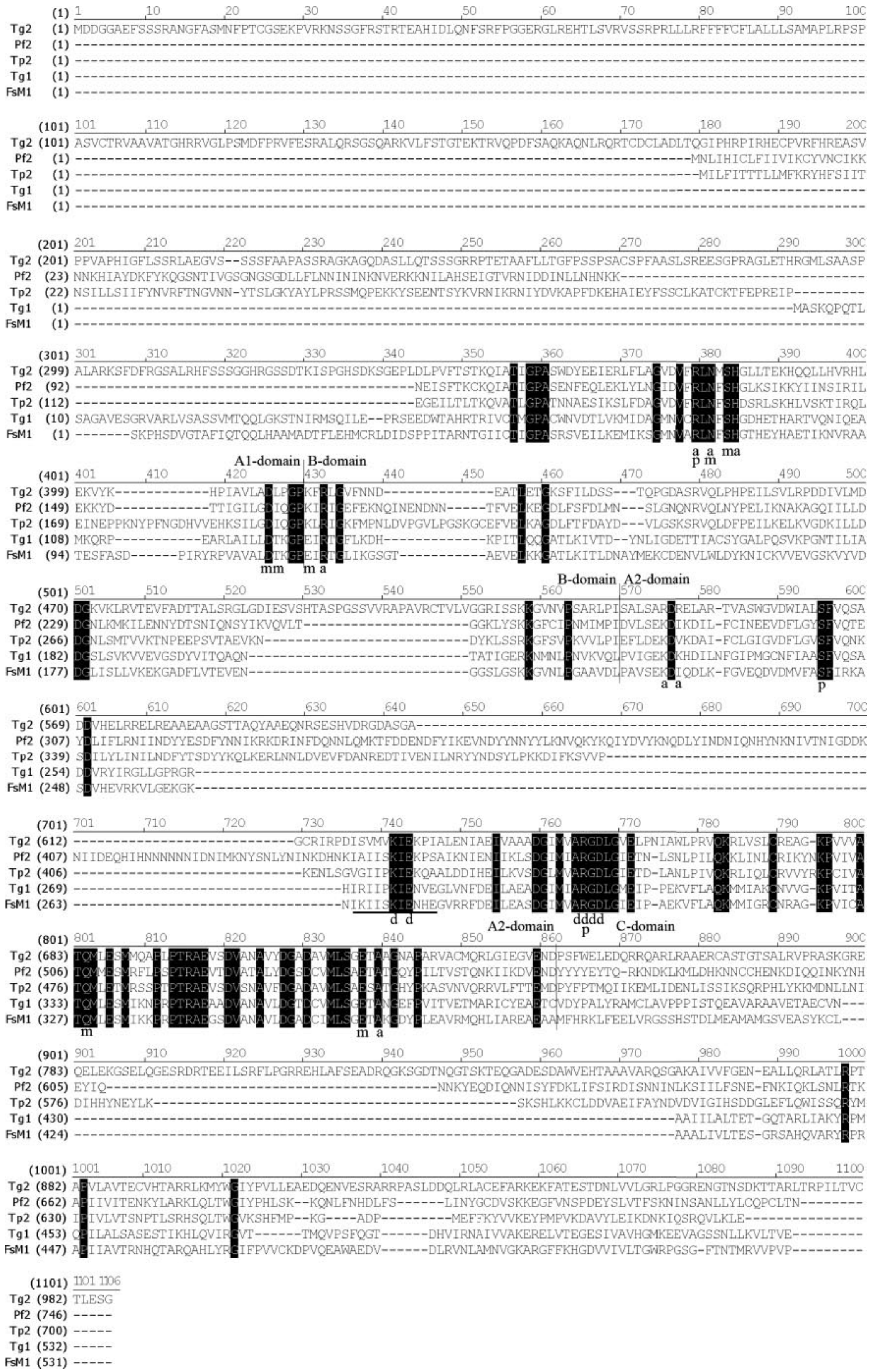
Tg2
Pf2
Tp2
Tg1
FsM1
A1-domain
B-domain
B-domain
A2-domain
A2-domain
C-domain

Stacked images were collected using an Olympus IX70 inverted microscope equipped with a 100-watt Hg-vapor lamp with appropriate barrier/emission filters. Images were captured with a CoolSNAP Hi Res CCD camera (Photometrics, AZ) and DeltaVision softWoRx software (Applied Precision, WA). All images were subjected to three-dimensional rendering using DeltaVision softWoRx.

RESULTS

Gene Organization, Functional Motifs, and Phylogenetic Analysis of TgPyKII—We cloned a second pyruvate kinase isozyme gene from *T. gondii, Tg*PyKII, using EST data bases, cDNA library screening, and rapid amplification of cDNA ends. A BLAST search of the cDNA sequence in ToxoDB (18) identified the gene model TgTigrScan_6611 in chromosome III, consisting of two exons (1092 and 1871 bp) and an intron (764 bp) that encodes 988 amino acids with a calculated molecular mass of 106,837 Da and a pI of 8.77. BLASTP search shows that *Tg*PyKII is highly homologous to pyruvate kinases from α-proteobacteria with >40% identity and >50% similarity. Multiple sequence alignments with crystallized pyruvate kinases (35–37) show that *Tg*PyKII has a long N-terminal extension before the conserved region beginning at aa 345 (Fig. 1).

Compared with the pyruvate kinase domain structure consisting of A_1, A_2, B, and C domains, three unique insertions in the middle of domain B, A_2, and C (37), are present (Fig. 1). Both *Tg*PyKI and *Tg*PyKII contain a pyruvate kinase signature (PROSITE; PS00110) (Fig. 1, *line*) as well as consensus motifs for pyruvate kinase, including binding sites of ADP, PEP, and divalent cations (Fig. 1, *a*, *p*, *d*, respectively). *Tg*PyKI possesses all the conserved monovalent cation-binding sites (Fig. 1, *m*). In contrast, in *Tg*PyKII, two binding sites Thr^{113} and Glu^{117} in *Felis catus* pyruvate kinase are substituted by Leu^{412} and Lys^{416}, respectively. These substitutions are a common feature of monovalent cation-independent pyruvate kinases (38–40). Furthermore, the presence of Glu^{868} in *Tg*PyKII, conserved among enzymes that are insensitive to the pyruvate kinase activator, fructose 1,6-diphosphate (39), suggests that *Tg*PyKII is not activated by fructose 1,6-diphosphate.

*Tg*PyKII has overall amino acid sequence identity of 32% to *Tg*PyKI. Unlike *Tg*PyKII, *Tg*PyKI shows high homology to pyruvate kinases in other apicomplexan parasites and plants. Phylogenetic tree indicates that *Tg*PyKI is closely related to plant cytosolic pyruvate kinases along with pyruvate kinases from apicomplexan parasites such as *Cryptosporidium parvum* (EAK88569), *Plasmodium falciparum* (CAG25081), and *Theileria parva* (529.m04777) (Fig. 2). In contrast, *Tg*PyKII clusters with proteobacteria pyruvate kinases, along with two isozymes from apicomplexan parasites *P. falciparum* (AAG35560) and *T. parva* (529.m04771) (Fig. 2). These results suggest a different evolutionary origin of the two isozymes in *T. gondii,* a probable plant/algal origin of *Tg*PyKI and a probably proteobacterial origin of *Tg*PyKII.

Enzymatic Activity of Recombinant and Native TgPyKII Proteins—Conserved region of *Tg*PyKII (*Tg*PyKII-(293–988)) was expressed in *E. coli* as a fusion protein with glutathione *S*-transferase, which was removed by PreScission protease (Amersham Biosciences) digestion. SDS-PAGE detected the predicted size of 77 kDa for purified recombinant protein (Fig. 3*A*). The purified recombinant protein is shown to catalyze the pyruvate kinase reaction. The pH optimum of *Tg*PyKII activity is at pH 8.5, and more than 80% of the maximal activity is observed between pH 8.0 and pH 9.5 (data not shown). At pH 7.0, the optimal pH of *Tg*PyKI (11), the activity of *Tg*PyKII is 50% of the maximal activity. The enzyme was stable when stored in buffer containing 20 mM Tris-Cl, pH 7.0, and 30% glycerol for 1 week at 4 °C. The enzyme activity remained stable after one freeze-thaw cycle.

Most pyruvate kinases require monovalent cations, show allosteric properties for PEP binding, and are regulated by phosphorylated sugars. Interestingly, amino acid sequence (Fig. 1) suggests that monovalent cations are not required for *Tg*PyKII activity, which was confirmed by biochemical assay. Also, the saturation curve is hyperbolic with the substrate PEP. The K_m value for PEP is 0.116 ± 0.011 mM. Although most pyruvate kinases prefer ADP as a phosphate recipient, the k_{cat}/K_m values for GDP and IDP are 337- and 114-fold higher, respectively, than that for ADP (Table 1). Moreover, the substrates GDP and IDP exert inhibitory activities (Table 1). The specific activity at 0.5 mM CDP and UDP was less than 10% that at 0.5 mM GDP. These data indicate that GDP is a preferred substrate for *Tg*PyKII. Other possible effectors were tested at sub-saturating concentrations of PEP and GDP (0.2 and 0.1 mM, respectively). None of the following compounds influence *Tg*PyKII activity: fructose 1,6-diphosphate, glucose 6-phosphate, fructose 6-phosphate, glucose 1-phosphate, ribose 5-phosphate, ATP, ITP, AMP, His, Ser, Ala, Glu, Gln, Thr, Met, Gly, Ile, Asn, Cys, Pro, Arg, Lys, Phe, Trp, Leu, Asp, Val (1 mM each), Tyr (0.5 mM), 0.1 mM acetyl-CoA. Only 0.1 mM GTP reduces the V_{max} by 10 ± 1%.

To examine native *Tg*PyKII activity, we performed subcellular fractions of *T. gondii* tachyzoite cells. *Tg*PyKI and -II activities were distinguished based on their pH optimum (7.0 *versus* 8.5, respectively), requirement for the monovalent cation, and phosphate recipient specificity (ADP *versus* GDP) (Table 2). As *Tg*PyKI requires K^+ for the activity, *Tg*PyKI does not show any activity in the standard assay condition for *Tg*PyKII lacking K^+. In the standard assay condition for *Tg*PyKI, *Tg*PyKII shows less than 1/100 of its *Tg*PyKII activity. Although *Tg*PyKI activity is detected only in cytosolic fractions as reported previously (10), *Tg*PyKII activity is exclusively associated with membranous

FIGURE 1. **Amino acid sequence alignment of *T. gondii* pyruvate kinase II with four pyruvate kinases from other species.** Accession numbers for the sequence data shown are as follow: *Tg2*, *T. gondii* isozyme II (this study; AB118155); *Pf2*, *P. falciparum* isozymes II (AAN35560); *Tp2*, *T. parva* isozyme II (529.m04771); *Tg1*, *T. gondii* isozymes I (BAB47171); *FsM1*, *F. catus* isozyme M1 (P11979). Identical residues are highlighted in *black*. *Vertical lines* indicate the dividing line of four three-dimensional domains (*N, A1, A2, B, C*) of pyruvate kinase as described previously (37). A *horizontal line* indicates the pyruvate kinase signature sequence (PROSITE, PS00110; *p* indicates PEP-binding sites; *a* indicates ADP-binding sites; *d* indicates divalent cation-binding sites; *m* indicates monovalent cation-binding sites; *dashes* indicates gaps in the alignment.

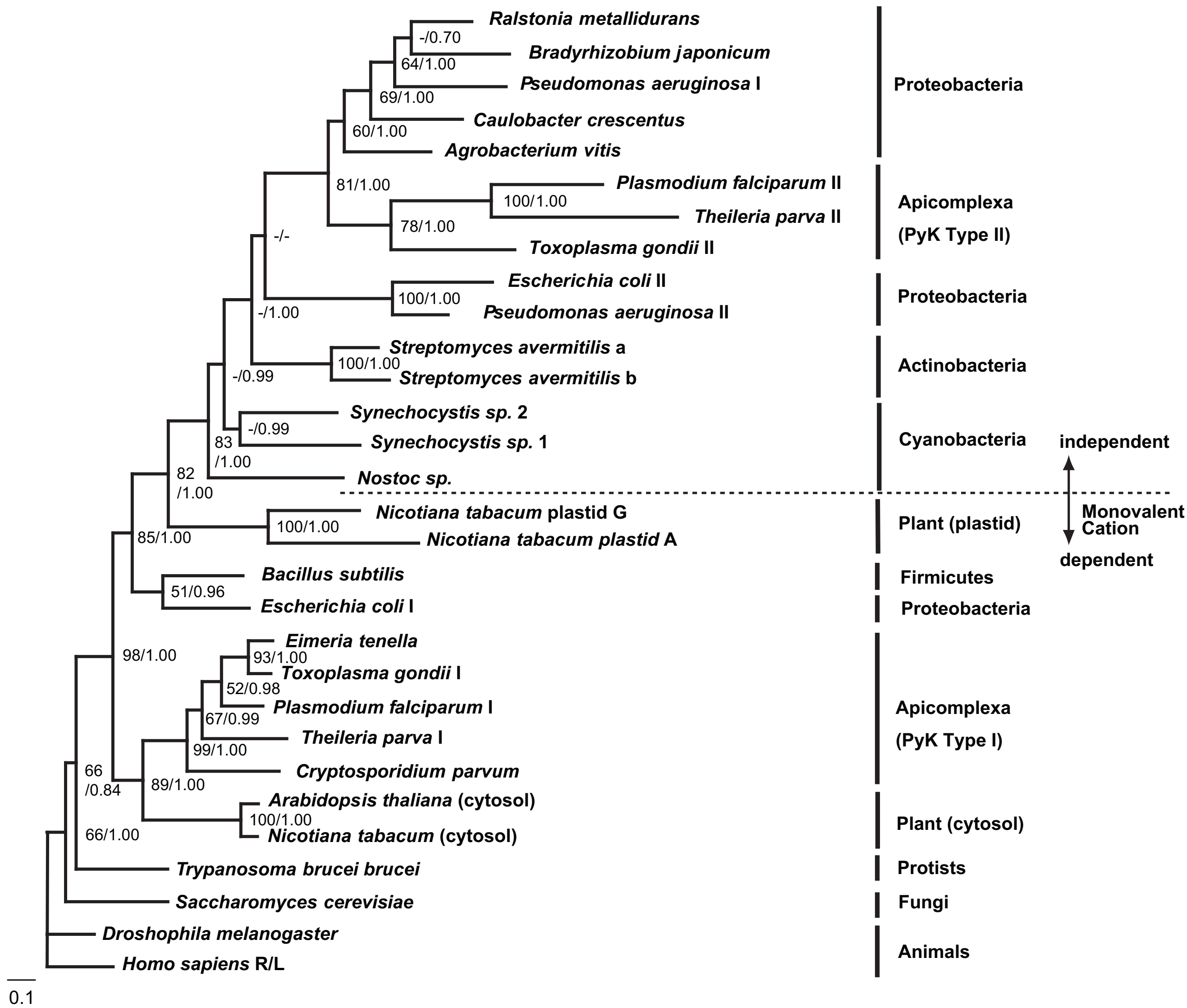

FIGURE 2. **Phylogenetic tree of pyruvate kinase constructed based on the deduced amino acid sequences of pyruvate kinase genes of 20 taxa.** Only evolutionarily conserved alignment regions (~230 amino acid characters) were used for phylogenetic inference by the Bayesian inference and maximum likelihood methods. The tree shown is the consensus tree estimated by Bayesian analysis with the JTT matrix. Maximum likelihood distance tree was also carried out. *Numbers* at branches are bootstrap values for the maximum likelihood protein distance analysis (100 replicates, >50 were indicated) and Bayesian posterior probabilities (>0.5 were indicated). *Bar* indicates the substitution. The accession numbers in GenBank™ for all pyruvate kinase sequences used for phylogenetic analysis are as follows: *Drosophila melanogaster* (AAC16244); *Homo sapiens* R/L (AAA60104);*Saccharomyces cerevisiae* (CAA32573); *Trypanosoma brucei brucei* (P30615); *C. parvum* (EAK88569); *P. falciparum* (I, CAG25081; II, AAN35560); *T. gondii* (I, BAB47171; II, in this article); *T. parva* (I, 529.m04777; II, 529.m04771); *A. thaliana* (cytosol, BAB10006); *Nicotiana tabacum* (cytosol, CAA82628; plastid A, CAA82222; plastid G, CAA82223); *Streptomyces avermitilis* (a, BAC70536; b, BAC73928);*Synechocystis* sp. (1, BAA10621; 2, BAA17574); *Nostoc* sp. PCC7120 (BAB74263); *Bacillus subtilis* (P80885); *E. coli* (type I, AAA24392; type II, AAA24473); *Pseudomonas aeruginosa* (I, NP_250189; II, NP_253019); *Bradyrhizobium japonicum* (NP_773778); *Ralstonia metallidurans* (ZP_00275735); *Caulobacter crescentus* (NP_420856); and *Agrobacterium vitis* (Q44473).

fraction, the purity of which is confirmed by mitochondrial succinate dehydrogenase activity. The procedure of solubilization of membranous fraction did not have any detrimental impact on the activity of recombinant *Tg*PyKII. Thus, *Tg*PyKII is localized to membrane-bound compartments.

Localization of TgPyKII and Analysis of Its Subcellular Localization Signals—Anti-*Tg*PyKII antibody was generated to detect endogenous *Tg*PyKII protein in *T. gondii* tachyzoite cells. Western blot analysis shows that anti-*Tg*PyKII antibody specifically detects the recombinant *Tg*PyKII protein (Fig. 3*B*, *lane 1*), not the recombinant *Tg*PyKI protein (Fig. 3*B*, *lane 2*) and the host cell (data not shown). A single band of ~75 kDa was detected by this antibody in whole lysate of tachyzoite cells (Fig. 3*C*). To analyze the localization of native *Tg*PyKII protein in tachyzoite cells, FNR_L-YFP-HA parasites (labeling the apicoplast) were labeled with MitoTracker Red (labeling the mitochondrion) and *Tg*PyKII antibody (Fig. 4). Endogenous *Tg*PyKII (Fig. 4, *blue*) localizes to the apicoplast (Fig. 4, *green*) and the mitochondrion (Fig. 4, *red*) along with apical side of endoplasmic reticulum (ER) (Fig. 4, *arrowheads*), which was confirmed with a co-localization experiment using ER marker (data not shown).

Multiple sequence alignments of pyruvate kinases (Fig. 1) show that *Tg*PyKII has a long N-terminal unconserved extension containing five possible start codons (Fig. 5*A*, *red bold*), which may acts as subcellular localization signal(s). TargetP,

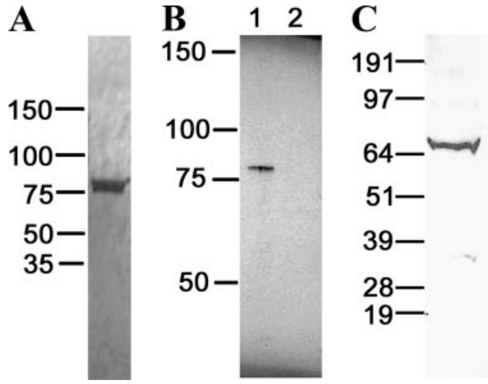

FIGURE 3. **Recombinant protein expression and native antibody of *Tg*PyKII.** *A,* SDS-PAGE of 3 μg of purified recombinant *Tg*PyKII with the N-terminal extension truncated. Electrophoresis was carried out on 5–10% gradient polyacrylamide gel. The protein was detected by Coomassie Brilliant Blue R-250 staining. *B* and *C,* specificity of anti-*Tg*PyKII IgG shown by Western blot analysis. *B,* 3 ng of recombinant *Tg*PyKII (*lane 1*) and *Tg*PyKI (*lane 2*). *C,* 1×10^8 *T. gondii* tachyzoite whole cell lysate. Molecular mass is expressed in kDa.

TABLE 1

Kinetic parameters of *T. gondii* pyruvate kinase I and II for nucleoside diphosphates

Substrate	Enzyme	K_m	K_i[a]	k_{cat}[b]	k_{cat}/K_m
		mM	mM	s^{-1}	$mM^{-1}\,s^{-1}$
ADP	*Tg*PyKI[c]	0.180 ± 0.110		174	966
	*Tg*PyKII[d]	7.99 ± 0.44		47.6 ± 1.4	6
GDP[e]	*Tg*PyKII	0.0544 ± 0.0061	1.68 ± 0.18	110 ± 4	2020
IDP[f]	*Tg*PyKII	0.193 ± 0.014	4.89 ± 0.49	131 ± 4	681

[a] GDP and IDP exhibited substrate inhibition.
[b] k_{cat} values were calculated as V_{max} divided by molar enzyme concentration.
[c] Cited and calculated from data in Maeda *et al.* (11).
[d] ADP concentration assayed was 1 to 10 mM.
[e] GDP concentration assayed was 0.025 to 2 mM.
[f] IDP concentration assayed was 0.05 to 4 mM.

TABLE 2

Total activity of enzymes in subcellular fractions of *T. gondii* tachyzoites

Fraction	Total activity[a] (units/10^{10} tachyzoite cells)		
	Pyruvate kinase activity		SDH[d]
	*Tg*PyKI[b]	*Tg*PyKII[c]	
Cytosolic fraction	153 ± 7	<0.01	<0.005
Membranous fraction	<0.01	0.920 ± 0.190	0.854 ± 0.088

[a] All values were determined by three independent experiments. One unit of enzyme activity is defined as the amount of enzyme resulting in the consumption of 1 μmol of NADH/min (pyruvate kinase) or 2 μmol of ferricyanide/min (succinate dehydrogenase).
[b] Shown is the activity under optimal conditions and substrate for *T. gondii* pyruvate kinase I (1 mM PEP, 1 mM ADP, 10 mM $MgSO_4$, 100 mM KCl_2, pH 7.0).
[c] Shown is the activity under optimal conditions and substrate for *T. gondii* pyruvate kinase II (1 mM PEP, 0.5 mM GDP, 25.5 mM $MgCl_2$, pH 8.5).
[d] SDH means succinate dehydrogenase.

SignalP, and ChloroP were used to predict the presence of signals in N-terminal 357 amino acids (Fig. 5). SignalP 3.0 (21) with 100 truncation max residues was used to predict the presence of canonical secretory signal peptide (SP) or anchor (SA) in translation products from five possible start codons (Fig. 5, *ocher*). Although SignalP-NN, the neural networks based algorithm, predicted a weak SP cleavage site between aa 92 and 93 for the 1st Met protein product, SignalP-HMM (41), the hidden Markov model algorithm, highly favors SA ($p = 0.995$). The same prediction was observed for the 2ndMet product. The Kyte-Doolittle hydrophobicity profile showed the presence of a strong hydrophobic stretch between aa ~75 and 92 corresponding the prediction of SignalP (Fig. 5*B*). ChloroP (23) predicted possible plastid transit peptides (pTPs) for translation products from the 1st, 3rd, and 5th Met (Fig. 5, *green*). The predicted pTP cleavage sites for the 1st, 3rd, and 5th Met products are between aa 69 and 70, aa 159 and 160, and aa 309 and 310, respectively (note that amino acid positions are counted from the position of 1st Met). TargetP (20) predicted the presence of mitochondrial targeting peptides (mTPs) for translation products from 3rd, 4th, and 5th Met (Fig. 5, *magenta*). The predicted mTP cleavage sites are between aa 140 and 141 for the 3rd and 4th Met products and aa 316 to 317 for the 5th Met product. Summary of the possible signal sequences for various protein products is shown in Fig. 5*C*.

To determine whether the N-terminal unconserved region of *Tg*PyKII can function as a dual targeting signal to the mitochondrion and the apicoplast, YFP-HA was fused to the N-terminal 357 aa of *Tg*PyKII (*Tg*PyKII1stM-(1–357)-YFP-HA) and expressed in tachyzoites (Fig. 6*A*). YFP labeling co-localizes to both the apicoplast (Fig. 5*A*, *blue*) and the mitochondrion (Fig. 5*A*, *red*), suggesting that this region is responsible for proper localization of *Tg*PyKII. Because this N-terminal extension contains five possible start codons, the dual targeting of *Tg*PyKII1stM-(1–357)-YFP-HA could result from one protein targeted to both organelles or two proteins targeted to each individual organelle. To answer this, we fused YFP-HA to N-terminal unconserved regions starting from downstream possible start codons (at aa positions 19 for 2nd Met, 93 for 3rd Met, 122 for 4th Met, and 293 for 5th Met) and expressed in tachyzoites. YFP labeling of *Tg*PyKII2ndM-(19–357)-YFP-HA (Fig. 6*B*) and *Tg*PyKII3rdM-(93–357)-YFP-HA (Fig. 6*C*) is localized only to the mitochondrion, whereas that of *Tg*PyKII4thM-(122–357)-YFP-HA and *Tg*PyKII5thM-(293–357)-YFP-HA is localized to cytosol (data not shown). These results suggest that the dual targeting of *Tg*PyKII-1stM-(1–357)-YFP-HA could result from one protein product (*i.e.* 1st Met product targeted to both organelles) or two protein products (*i.e.* 1st Met product targeted to the apicoplast and either 2nd Met or 3rd Met product targeted to the mitochondrion). To determine whether there are one or two products responsible for the dual targeting, we performed site-directed mutagenesis changing 2nd Met or 3rd Met to Ala in *Tg*PyKII1stM-(1–357)-YFP-HA construct and expressed them in tachyzoites. Although *Tg*PyKII[2ndM19A]-YFP-HA targets YFP-HA to the apicoplast and the mitochondrion (Fig. 7*A*), *Tg*PyKII[3rdM93A]-YFP-HA targeted only to the apicoplast (Fig. 7*B*). These results suggest that two protein products are responsible for dual targeting, 1st Met product for the apicoplast and the 3rd Met product for the mitochondrion.

DISCUSSION

We characterized a novel pyruvate kinase isozyme in *T. gondii*, *Tg*PyKII, with unique enzymatic properties. pH optimum for *Tg*PyKII activity is at 8.5, and more than 80% of the maximal activity was observed even at pH 9.0, more alkalinic than the pH optima reported for any other pyruvate kinases (5.5–8.0) (42,

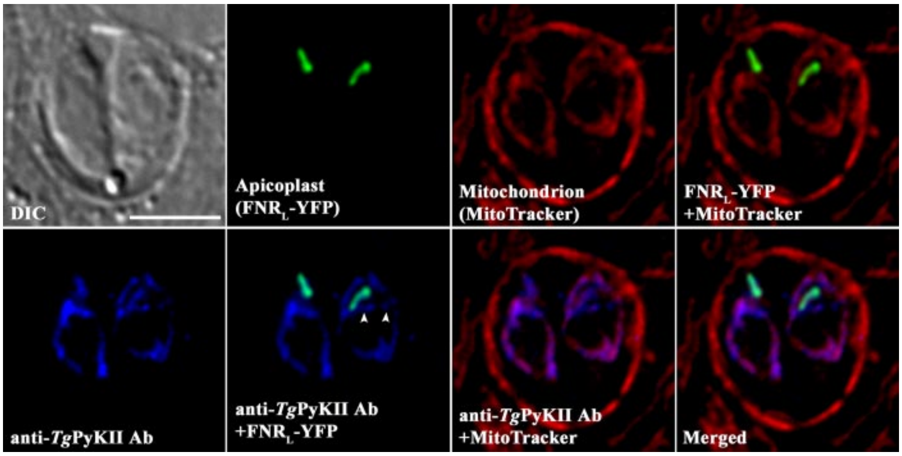

FIGURE 4. **Apicoplast and mitochondrial localization of native *Tg*PyKII in *T. gondii* tachyzoite.** Parasites stably expressing p*tub*FNR$_L$-YFP-HA (labeling apicoplast, *green*) were stained with MitoTracker Red CMXRos (*red*) and anti-*Tg*PyKII antibody (*blue*). Note that in addition to apicoplast and mitochondrion, *Tg*PyKII antibody localizes to apical ER (*arrowheads*) that may indicate a possible exit site of *Tg*PyKII from ER. *Scale bar*, 5 μm. *DIC*, differential interference contrast.

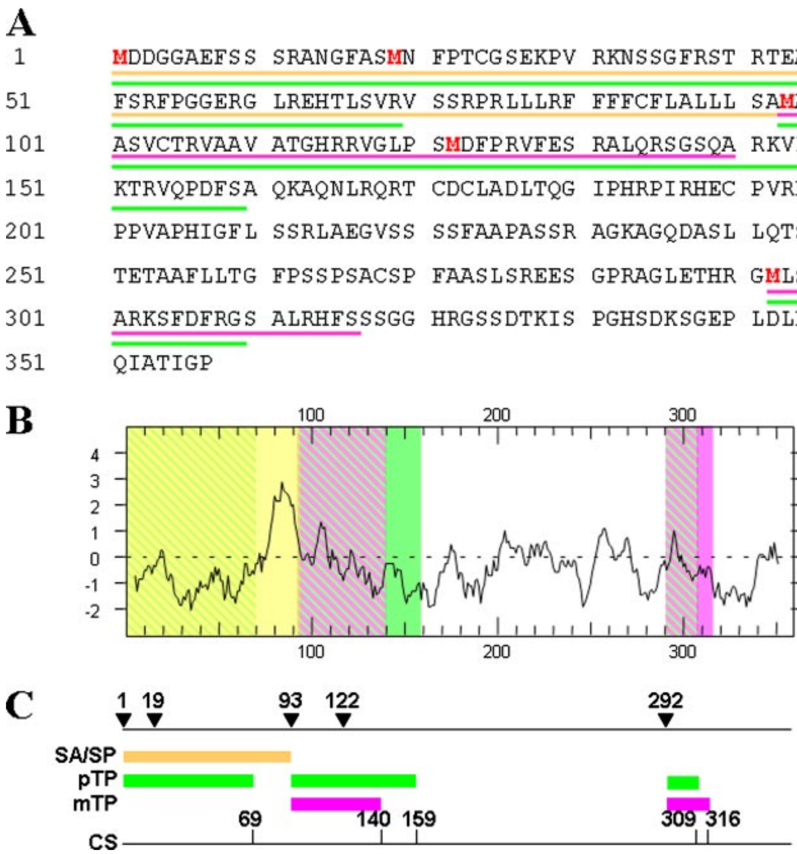

FIGURE 5. **Signal prediction of the N-terminal extension of *Tg*PyKII in *T. gondii*.** *A,* N-terminal 357 amino acid sequence of *Tg*PyKII. Methionines are highlighted in *red*. *Colored underlines* are location of predicted signals (see below for color codes). *B,* Kyte-Doolittle hydrophobicity plot of the N-terminal extension of *Tg*PyKII showing a strong hydrophobic stretch between aa 75 and 92. *Color-shaded* regions are location of predicted signals (see below for color codes). Colors are *hatched* in regions where signals are overlapped. *C,* summary of predicted signals. *Inverted black triangles* indicate the location of each methionine with amino acid position listed above. The *numbers* above the *tick mark* indicate the amino acid position before the predicted signal cleavage sites. *Colored boxes* are location of predicted signals. Predicted SA/SP, *ocher*; predicted plastid transit peptide (pTP), *green*; predicted mitochondrion targeting peptide (mTP), *magenta*; *CS*, cleavage site.

43). Although the actual physiological pH value of the apicoplast or the mitochondrion in *T. gondii* is still unknown, several enzymes localized in the apicoplast in *P. falciparum* (44), plastid in barley roots (45), or mitochondrion in yeast (46) and *Arabidopsis thaliana* (47) have alkaline pH optima like *Tg*PyKII. It is also possible, however, the maximal activity of *Tg*PyKII may not be necessary in parasite survival.

Although ADP is generally considered as the phosphate recipient of pyruvate kinase in glycolysis, pyruvate kinase activity is relatively nonspecific in its utilization of purine and pyrimidine nucleotide substrates (48). Some bacterial pyruvate kinases prefer GDP over ADP (5, 49, 50), but their k_{cat}/K_m (or V_{max}/K_m) ratio for GDP is only 10–20-fold higher than that for ADP. However, in case of *Tg*PyKII, GDP is preferred over ADP as a phosphate recipient with 377-fold higher k_{cat}/K_m (or V_{max}/K_m) ratio, suggesting GDP as a sole phosphate recipient.

Pyruvate kinases are generally activated by sugar phosphates and bind PEP allosterically (51). Albeit fructose 1,6-diphosphate is a typical allosteric activator, some pyruvate kinases use other activators such as fructose 2,6-diphosphate (52) in trypanosomatid protozoans and glucose 6-phosphate in *Eimeria tenella* (53), *Mycobacterium smegmatis* (54), *Strepotcoccus mutans* (49), and *Tg*PyKI (11). Our study shows that *Tg*PyKII is not activated by fructose 1,6-diphosphate and other known activators for pyruvate kinase such as sugar phosphates, and consistently, it does not show allosteric binding to PEP. Thus *Tg*PyKII does not seem to have regulatory properties like as *Tg*PyKI.

Pyruvate kinase can be classified by the requirement for a monovalent cation. Structural analysis (55), point mutation analysis (38, 39), and phylogenetic analysis (40) suggest that (Thr^{113} and Glu^{117}) and (Leu/Ile^{113} and Ser/Lys^{117}) (numbers in *F. catus* pyruvate kinase) are responsible for monovalent cation dependence and independence, respectively. Monovalent cation-independent isozymes (type II) exist in prokaryotes like actinobacteria, cyanobacteria, and proteobacteria, whereas monovalent cation-dependent isozymes (type I) exist in mammals, plants, and fungi (Fig. 2). In prokaryotes, *Clostridium perfringens, Leptospira interrogans,*

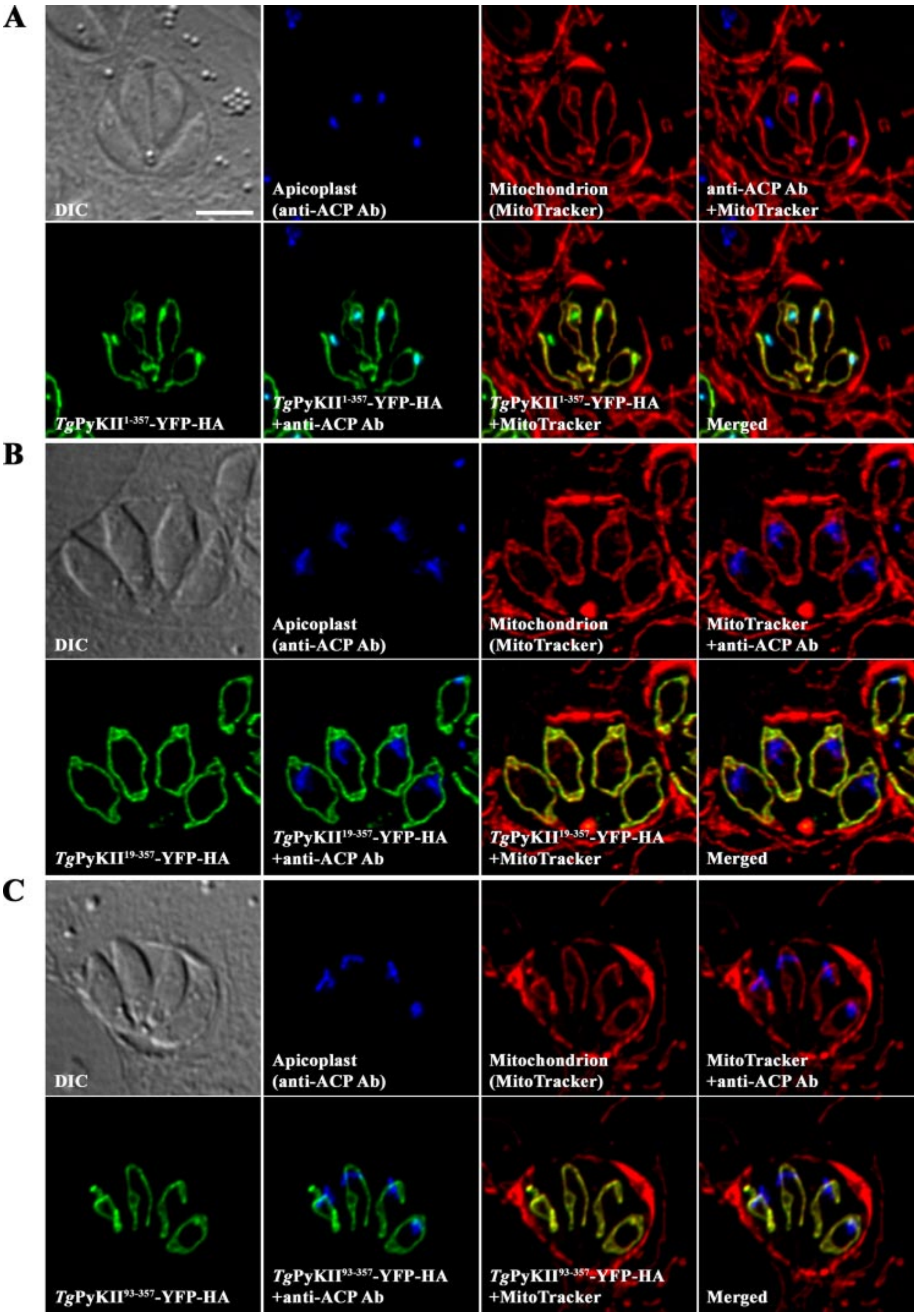

FIGURE 6. **Localization of *Tg*PyKII1stM-(1–357)-YFP-HA, *Tg*PyKII2ndM-(19–357)-YFP-HA, and *Tg*PyKII3rdM-(93–357)-YFP-HA.** Parasites were transfected with *Tg*PyKII1stM-(1–357)-YFP-HA (*A*), *Tg*PyKII2ndM-(19–357)-YFP-HA (*B*), or *Tg*PyKII3rdM-(93–357)-YFP-HA (*C*) under tubulin (in these panels) or dihydrofolate reductase (not shown) promoters and labeled with MitoTracker Red CMXRos (labeling mitochondrion, *red*) and anti-ACP antibody (labeling apicoplast, *blue*). The same phenotype was observed for different promoters. *Scale bar*, 5 μm. *DIC*, differential interference contrast.

E. coli, Vibrio cholerae, and *Salmonella typhimurium* possess both types. In eukaryotes, so far only apicomplexan parasites, *T. gondii* (in this study), *P. falciparum* (56), *Theileria annulata* (contig 1823 and contig13), and *T. parva* (529.m04777 and 529.m0471) possess both types. Phylogenetic analysis shows that Apicomplexan type I pyruvate kinase clusters with plants and apicomplexan type II pyruvate kinase with proteobacteria (Fig. 2), suggesting that monovalent cation-independent isozymes (type II) in apicomplexan parasites are of proteobacterial origin and obtained by horizontal gene transfer (Fig. 2). *Neospora caninum* possibly contains the proteobacteria-like pyruvate kinase isozyme (contig5134), but the full sequence has not been determined. The proteobacteria-like pyruvate kinase isozyme is not found in the complete genome sequence data base of *C. parvum,* which possesses a reduced mitochondria (mitome) but lacks the apicoplast. Genome sequencing of *Eimeria tenella* has not been completed at this time.

Another striking feature of *Tg*PyKII is its dual localization to the apicoplast and mitochondrion as there is no documented evidence of a pyruvate kinase present in the mitochondrion in any other organism. In plants, although proteins are normally transported to chloroplasts or mitochondria from cytoplasm using organelle-specific N-terminal targeting signals, pTP or mTP, respectively, proteins can be dually targeted to both organelles by two types of signals as follows: (i) a twin presequence from alternative transcription start, alternative translation start, or alternative exons results in two proteins, one targeted to the chloroplast and the other to the mitochondrion; and (ii) an ambiguous presequence results in one protein targeted to both organelles (57). In *T. gondii*, although mitochondrial proteins use a classical mTP, proteins are targeted to the apicoplast, a secondary endosymbiotic plastid, using a unique N-terminal bipartite signal consisting of a secretory signal peptide (SP) followed by pTP (17, 58). Yet recently, a superoxide dismutase (*Tg*SOD2) having a typical apicoplast bipartite signal is reported to localize to both apicoplast and mitochondrion as a single gene product (59). In this study, we showed that *Tg*PyKII possesses an N-terminal extension, which contains five possible start codons and probable SA/SP, pTP, and mTP (Fig. 5). Using fluorescent reporter fused to N-terminal 357 aa from the 1st Met (*Tg*PyKII1stM-(1–357)-YFP-HA), we prove that this region is responsible for localization to the apicoplast and the mitochondrion. Fluorescent fusions from 2nd and 3rd Met result in localization to the mito-

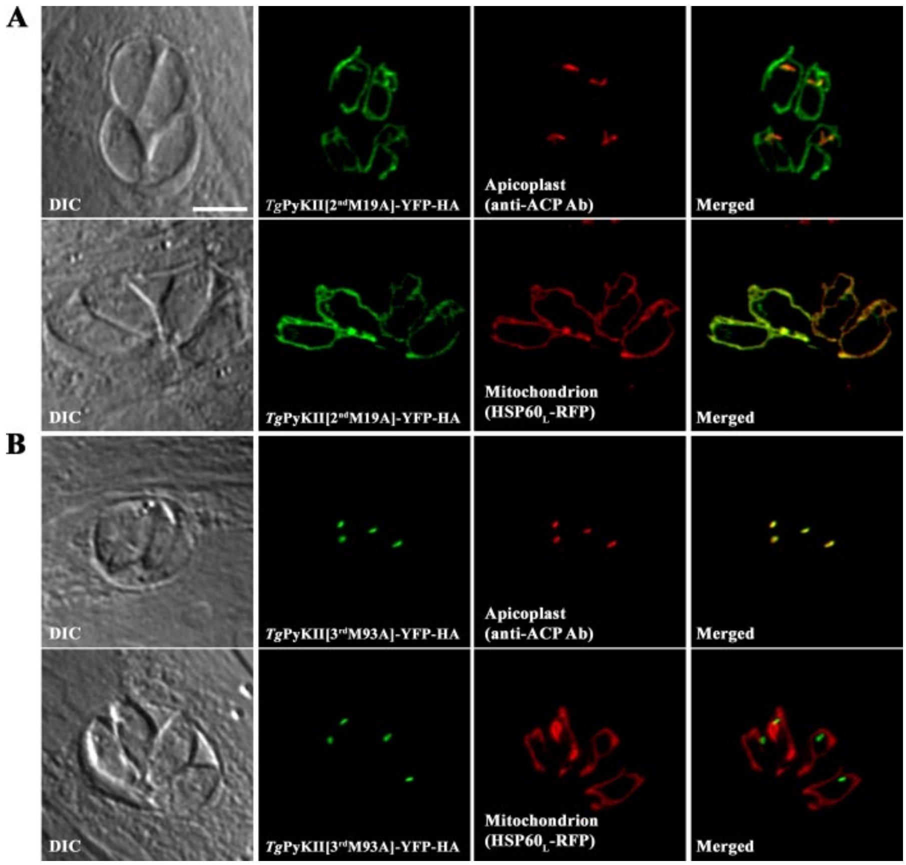

FIGURE 7. **Localization of *Tg*PyKII[2ndM19A]-YFP-HA and *Tg*PyKII[3rdM93A]-YFP-HA.** *A,* localization of *Tg*PyKII[2ndM19A]-YFP-HA. *Top panels*, wild type RH parasites transfected with p*minTg*PyKII[2ndM19A]-YFP-HA (*green*) and labeled with anti-ACP antibody (labeling apicoplast, *red*). *Bottom panels*, RH parasites stably expressing HSP60$_L$-RFP (labeling mitochondrion, *red*) transfected with p*minTg*PyKII[2ndM19A]-YFP-HA (*green*). *B,* localization of *Tg*PyKII[3rdM93A]-YFP-HA. *Top panels*, wild type RH parasites transfected with p*minTg*PyKII[3rdM93A]-YFP-HA (*green*) and labeled with anti-ACP antibody (labeling apicoplast, *red*). *Bottom panels*, RH parasites stably expressing HSP60$_L$-RFP (labeling mitochondrion, *red*) transfected with p*minTg*PyKII[3rdM93A]-YFP-HA (*green*). The same phenotype was observed for constructs under tubulin promoter. *Scale bar*, 5 μm. *DIC*, differential interference contrast.

chondrion only, suggesting that 1st Met product is responsible for apicoplast localization. *Tg*PyKII was predicted to have an SA/SP (with higher probability for SA) from aa 1 to 92 (Fig. 5, *ocher*) because of an unusual hydrophobic region rich in leucine and phenylalanine between aa 75 and 92. However, *Tg*PyKII2ndM-(19–357)-YFP-HA, despite containing this hydrophobic region, does not localize to the apicoplast, suggesting that 18 aa between the 1st and 2nd Met is necessary for proper translocation into the ER and thus the apicoplast. Site-directed mutagenesis analysis showed that 3rd Met translation product, not 2nd Met, in the N-terminal extension of *Tg*PyKII is responsible for the localization to the mitochondrion, consistent with the presence of mTP from 3rd Met (Fig. 5, *magenta*). Thus, unlike *Tg*SOD2, two translation products are responsible for dual localization of *Tg*PyKII, 1st Met product for the apicoplast and 3rd Met product for the mitochondrion. Further characterization of signals and signal cleavage sites has currently been carried out.

Type I monovalent cation-dependent isozymes in the apicomplexa lack an N-terminal extension, suggesting that, as in *Tg*PyKI, they localize in the cytosol. On the other hand, type II monovalent cation-independent isozymes with proteobacterial origin found in *P. falciparum, T. annulata,* and *T. parva* possess an N-terminal extension containing a typical bipartite apicoplast targeting signal. *P. falciparum* PyKII (AAN35560) does not have any internal methionines and was shown to localize only to the apicoplast by immunostaining using native antibody.[6] *T. parva* PyKII (529.m04771) has internal methionines and could be dual-localized like as *Tg*PyKII.

Although plant isozyme in plastids (60, 61) is a noncytosolic pyruvate kinase that functions in the glycolysis (62), noncytosolic pyruvate kinase found in the apicomplexan parasites may be involved in a unique metabolic pathway other than glycolysis, in which cytosolic pyruvate kinase plays a regulatory role. A plastidic sugar phosphate transporter was shown to localize to the apicoplast of *T. gondii* (16), which may suggest that triose sugars such as PEP could be transported from the cytosol to the apicoplast. Pyruvate dehydrogenase complex (59, 63, 64), enzymes in type II fatty acid synthesis (65, 66), and 1-deoxy-D-xylulose 5-phosphate synthesis (67) are localized in the apicoplast in *T. gondii*. Thus, in the apicoplast, *Tg*PyKII may function in supplying acetyl Co-A in cooperation with pyruvate dehydrogenase complex for fatty acid as well as 1-deoxy-D-xylulose 5-phosphate syntheses, as suggested in *P. falciparum* (68). Although *T. parva* does not possess FAS pathway in the apicoplast, PyKII in *T. parva* may contribute to the 1-deoxy-D-xylulose 5-phosphate pathway (69). The unique GTP supply role of *Tg*PyKII may contribute to provide an energy source for protein synthesis and a substrate for RNA synthesis in the apicoplast that has its own DNA (70).

To date, pyruvate kinase has not been identified in the mitochondria of any organism. As the substrate PEP can be provided from gluconeogenesis pathway through mitochondrial PEP carboxykinase (NCBI ID BAC02911), this unusual "short cut" might contribute to the rapid switching from gluconeogenesis to the oxidative phosphorylation. However, the fate of the product pyruvate is currently unknown, as pyruvate dehydrogenase complex does not localize in the mitochondrion (59, 64), whereas *T. gondii* tricarboxylic acid cycle is functional in the tachyzoite stage (71–73). The metabolic pathway connecting pyruvate with tricarboxylic acid cycle in the mitochondria in

[6] T. Maeda, T. Saito, O. Harb, D. S. Roos, A. Takeo, H. Suzuki, T. Tsuboi, T. Takeuchi, and T. Asai, unpublished data.

the apicomplexan parasites has been the unsolved question (34, 59, 63, 64). Although currently available data from biochemical and bioinformatics analyses do not provide explicit explanation for the role of *Tg*PyKII in the *T. gondii* mitochondrion, as the dual targeting to the apicoplast and mitochondrion can occur in previously unpredictable mechanisms in *T. gondii* (59 and in this study), further studies on experimental protein targeting may reconstruct metabolic pathways, and detailed information about the intraorganelle milieu will elucidate the physiological role of *Tg*PyKII in the mitochondrion.

REFERENCES

1. Dubey, J. P. (1993) in *Parasitic Protozoa* (Kreier, J. P., ed) pp. 5–56, Academic Press, San Diego
2. Fulton, J. D., and Spooner, D. F. (1960) *Exp. Parasitol.* **9,** 293–301
3. Boyer, P. D. (1962) in *The Enzymes* (Boyer, P. D., Lardy, H., and Myrback, K., eds) 2nd Ed., pp. 95–113, Academic Press, New York
4. Valentini, G., Chiarelli, L., Fortin, R., Speranza, M. L., Galizzi, A., and Mattevi, A. (2000) *J. Biol. Chem.* **275,** 18145–18152
5. Waygood, E. B., and Sanwal, B. D. (1974) *J. Biol. Chem.* **249,** 265–274
6. Waygood, E. B., Rayman, M. K., and Sanwal, B. D. (1975) *Can. J. Biochem.* **53,** 444–454
7. Plaxton, W. C. (1996) *Annu. Rev. Plant Physiol. Plant Mol. Biol.* **47,** 185–214
8. Saito, T., Maeda, T., Nakazawa, M., Takeuchi, T., Nozaki, T., and Asai, T. (2002) *Int. J. Parasitol.* **32,** 961–967
9. Peng, Z. Y., and Mansour, T. E. (1992) *Mol. Biochem. Parasitol.* **54,** 223–230
10. Denton, H., Roberts, C. W., Alexander, J., Thong, K. W., and Coombs, G. H. (1996) *FEMS Microbiol. Lett.* **137,** 103–108
11. Maeda, T., Saito, T., Oguchi, Y., Nakazawa, M., Takeuchi, T., and Asai, T. (2003) *Parasitol. Res.* **89,** 259–265
12. Bahl, A., Brunk, B., Crabtree, J., Fraunholz, M. J., Gajria, B., Grant, G. R., Ginsburg, H., Gupta, D., Kissinger, J. C., Labo, P., Li, L., Mailman, M. D., Milgram, A. J., Pearson, D. S., Roos, D. S., Schug, J., Stoeckert, C. J., Jr., and Whetzel, P. (2003) *Nucleic Acids Res.* **31,** 212–215
13. Hoffman, S. L., Subramanian, G. M., Collins, F. H., and Venter, J. C. (2002) *Nature* **415,** 702–709
14. Roos, D. S., Donald, R. G., Morrissette, N. S., and Moulton, A. L. (1994) *Methods Cell Biol.* **45,** 27–63
15. Asai, T., and Suzuki, Y. (1990) *FEMS Microbiol. Lett.* **60,** 89–92
16. Nishi, M. (2006) *Cell-cycle Regulation of Organelle Biogenesis and Apicoplast Protein Trafficking in Toxoplasma gondii.* Ph.D. thesis, University of Pennsylvania
17. Waller, R. F., Keeling, P. J., Donald, R. G., Striepen, B., Handman, E., Lang-Unnasch, N., Cowman, A. F., Besra, G. S., Roos, D. S., and McFadden, G. I. (1998) *Proc. Natl. Acad. Sci. U. S. A.* **95,** 12352–12357
18. Kissinger, J. C., Gajria, B., Li, L., Paulsen, I. T., and Roos, D. S. (2003) *Nucleic Acids Res.* **31,** 234–236
19. Hulo, N., Bairoch, A., Bulliard, V., Cerutti, L., De Castro, E., Langendijk-Genevaux, P. S., Pagni, M., and Sigrist, C. J. (2006) *Nucleic Acids Res.* **34,** D227–D230
20. Emanuelsson, O., Nielsen, H., Brunak, S., and von Heijne, G. (2000) *J. Mol. Biol.* **300,** 1005–1016
21. Nielsen, H., Engelbrecht, J., Brunak, S., and von Heijne, G. (1997) *Protein Eng.* **10,** 1–6
22. Bendtsen, J. D., Nielsen, H., von Heijne, G., and Brunak, S. (2004) *J. Mol. Biol.* **340,** 783–795
23. Emanuelsson, O., Nielsen, H., and von Heijne, G. (1999) *Protein Sci.* **8,** 978–984
24. Kyte, J., and Doolittle, R. F. (1982) *J. Mol. Biol.* **157,** 105–132
25. Chen, F., Mackey, A. J., Stoeckert, C. J., Jr., and Roos, D. S. (2006) *Nucleic Acids Res.* **34,** D363–D368
26. Li, L., Stoeckert, C. J., Jr., and Roos, D. S. (2003) *Genome Res.* **13,** 2178–2189
27. Thompson, J. D., Gibson, T. J., Plewniak, F., Jeanmougin, F., and Higgins, D. G. (1997) *Nucleic Acids Res.* **25,** 4876–4882
28. Felsenstein, J. (1989) *Cladistics* **5,** 164–166
29. Schmidt, H. A., Strimmer, K., Vingron, M., and von Haeseler, A. (2002) *Bioinformatics* (*Oxf.*) **18,** 502–504
30. Huelsenbeck, J. P., and Ronquist, F. (2001) *Bioinformatics* (*Oxf.*) **17,** 754–755
31. Ronquist, F., and Huelsenbeck, J. P. (2003) *Bioinformatics* (*Oxf.*) **19,** 1572–1574
32. Kahn, A., and Marie, J. (1982) *Methods Enzymol.* **90,** 131–140
33. Sibley, L. D., Niesman, I. R., Asai, T., and Takeuchi, T. (1994) *Exp. Parasitol.* **79,** 301–311
34. van Dooren, G. G., Stimmler, L. M., and McFadden, G. I. (2006) *FEMS Microbiol. Rev.* **30,** 596–630
35. Muirhead, H., Clayden, D. A., Barford, D., Lorimer, C. G., Fothergill-Gilmore, L. A., Schiltz, E., and Schmitt, W. (1986) *EMBO J.* **5,** 475–481
36. Mattevi, A., Valentini, G., Rizzi, M., Speranza, M. L., Bolognesi, M., and Coda, A. (1995) *Structure* (*Lond.*) **3,** 729–741
37. Rigden, D. J., Phillips, S. E., Michels, P. A., and Fothergill-Gilmore, L. A. (1999) *J. Mol. Biol.* **291,** 615–635
38. Laughlin, L. T., and Reed, G. H. (1997) *Arch. Biochem. Biophys.* **348,** 262–267
39. Jurica, M. S., Mesecar, A., Heath, P. J., Shi, W., Nowak, T., and Stoddard, B. L. (1998) *Structure* (*Lond.*) **6,** 195–210
40. Oria-Hernandez, J., Riveros-Rosas, H., and Ramirez-Silva, L. (2006) *J. Biol. Chem.* **281,** 30717–30724
41. Krogh, A., and Nielsen, H. (1998) in *Proceedings of the Sixth International Conference on Intelligent Systems for Molecular Biology (ISMB 6), Menlo Park, June 28–July 1, 1998*, pp. 122–130, AAAI Press, Menlo Park, CA
42. Saavedra, E., Olivos, A., Encalada, R., and Moreno-Sanchez, R. (2004) *Exp. Parasitol.* **106,** 11–21
43. Hattori, J., Baum, B. R., McHugh, S. G., Blakeley, S. D., Dennis, D. T., and Miki, B. L. (1995) *Biochem. Syst. Ecol.* **23,** 773–780
44. Dhanasekaran, S., Chandra, N. R., Chandrasekhar Sagar, B. K., Rangarajan, P. N., and Padmanaban, G. (2004) *J. Biol. Chem.* **279,** 6934–6942
45. Esposito, S., Carfagna, S., Massaro, G., Vona, V., and Di Martino Rigano, V. (2001) *Planta* **212,** 627–634
46. Jault, J. M., Di Pietro, A., Falson, P., and Gautheron, D. C. (1991) *J. Biol. Chem.* **266,** 8073–8078
47. Olejnik, K., Murcha, M. W., Whelan, J., and Kraszewska, E. (2007) *FEBS J.* **274,** 4877–4885
48. Plowman, K. M., and Krall, A. R. (1965) *Biochemistry* **4,** 2809–2814
49. Abbe, K., and Yamada, T. (1982) *J. Bacteriol.* **149,** 299–305
50. Crow, V. L., and Pritchard, G. G. (1982) *Methods Enzymol.* **90,** 165–170
51. Munoz, M. E., and Ponce, E. (2003) *Comp. Biochem. Physiol. B. Biochem. Mol. Biol.* **135,** 197–218
52. van Schaftingen, E., Vandercammen, A., Detheux, M., and Davies, D. R. (1992) *Adv. Enzyme Regul.* **32,** 133–148
53. Denton, H., Brown, S. M., Roberts, C. W., Alexander, J., McDonald, V., Thong, K. W., and Coombs, G. H. (1996) *Mol. Biochem. Parasitol.* **76,** 23–29
54. Kapoor, R., and Venkitasubramanian, T. A. (1981) *Biochem. J.* **193,** 435–440
55. Larsen, T. M., Laughlin, L. T., Holden, H. M., Rayment, I., and Reed, G. H. (1994) *Biochemistry* **33,** 6301–6309
56. Gardner, M. J., Hall, N., Fung, E., White, O., Berriman, M., Hyman, R. W., Carlton, J. M., Pain, A., Nelson, K. E., Bowman, S., Paulsen, I. T., James, K., Eisen, J. A., Rutherford, K., Salzberg, S. L., Craig, A., Kyes, S., Chan, M. S., Nene, V., Shallom, S. J., Suh, B., Peterson, J., Angiuoli, S., Pertea, M., Allen, J., Selengut, J., Haft, D., Mather, M. W., Vaidya, A. B., Martin, D. M., Fairlamb, A. H., Fraunholz, M. J., Roos, D. S., Ralph, S. A., McFadden, G. I., Cummings, L. M., Subramanian, G. M., Mungall, C., Venter, J. C., Carucci, D. J., Hoffman, S. L., Newbold, C., Davis, R. W., Fraser, C. M., and Barrell, B. (2002) *Nature* **419,** 498–511
57. Peeters, N., and Small, I. (2001) *Biochim. Biophys. Acta* **1541,** 54–63
58. Roos, D. S., Crawford, M. J., Donald, R. G., Kissinger, J. C., Klimczak, L. J., and Striepen, B. (1999) *Curr. Opin. Microbiol.* **2,** 426–432
59. Pino, P., Foth, B. J., Kwok, L. Y., Sheiner, L., Schepers, R., Soldati, T., and Soldati-Favre, D. (2007) *Plos Pathog.* **3,** e115

60. Ireland, R. J., Luca, V. D., and Dennis, D. T. (1979) *Plant Physiol.* **63,** 903–907
61. Ireland, R. J., Luca, V. D., and Dennis, D. T. (1980) *Plant Physiol.* **65,** 1188–1193
62. Simcox, P. D., and Dennis, D. T. (1978) *Plant Physiol.* **61,** 871–877
63. Foth, B. J., Stimmler, L. M., Handman, E., Crabb, B. S., Hodder, A. N., and McFadden, G. I. (2005) *Mol. Microbiol.* **55,** 39–53
64. Crawford, M. J., Thomsen-Zieger, N., Ray, M., Schachtner, J., Roos, D. S., and Seeber, F. (2006) *EMBO J.* **25,** 3214–3222
65. Jelenska, J., Crawford, M. J., Harb, O. S., Zuther, E., Haselkorn, R., Roos, D. S., and Gornicki, P. (2001) *Proc. Natl. Acad. Sci. U. S. A.* **98,** 2723–2728
66. Mazumdar, J., Wilson, E. H., Masek, K., Hunter, C. A., and Striepen, B. (2006) *Proc. Natl. Acad. Sci. U. S. A.* **103,** 13192–13197
67. Wiesner, J., and Seeber, F. (2005) *Expert Opin. Ther. Targets* **9,** 23–44
68. Ralph, S. A., Van Dooren, G. G., Waller, R. F., Crawford, M. J., Fraunholz, M. J., Foth, B. J., Tonkin, C. J., Roos, D. S., and McFadden, G. I. (2004) *Nat. Rev. Microbiol.* **2,** 203–216
69. Goodman, C. D., and McFadden, G. I. (2007) *Curr. Drug Targets* **8,** 15–30
70. Wilson, R. J., Denny, P. W., Preiser, P. R., Rangachari, K., Roberts, K., Roy, A., Whyte, A., Strath, M., Moore, D. J., Moore, P. W., and Williamson, D. H. (1996) *J. Mol. Biol.* **261,** 155–172
71. Coombs, G. H., Denton, H., Brown, S. M., and Thong, K. W. (1997) *Adv. Parasitol.* **39,** 141–226
72. Melo, E. J., Attias, M., and De Souza, W. (2000) *J. Struct. Biol.* **130,** 27–33
73. Vercesi, A. E., Rodrigues, C. O., Uyemura, S. A., Zhong, L., and Moreno, S. N. (1998) *J. Biol. Chem.* **273,** 31040–31047